Oliveira, L. M. R. and Cardoso, A. J. M.: "Detection of transformer intermittent winding faults by the on-load exciting current Park's Vector approach," Proceedings of the 20th International Congress on Condition Monitoring and Diagnostic Engineering Management (COMADEM'07), pp. 263-272, Faro, Portugal, June 13-15, 2007.

DETECTION OF TRANSFORMER INTERMITTENT WINDING FAULTS BY THE ON-LOAD EXCITING CURRENT PARK'S VECTOR APPROACH

Luís M. R. Oliveira[1, 2] and A. J. Marques Cardoso[2]

[1] Escola Superior de Tecnologia da Universidade do Algarve; Campus da Penha;
P – 8005-139 Faro, Portugal
e-mail: lolivei@ualg.pt, phone: (+351) 289800100, fax: (+351) 289888405.
[2] Universidade de Coimbra, FCTUC/IT; Departamento de Engenharia Electrotécnica e de Computadores; Pólo II - Pinhal de Marrocos; P – 3030-290 Coimbra, Portugal
e-mail: ajmcardoso@ieee.org, phone: (+351) 239796232, fax: (+351) 239796247.

ABSTRACT

This paper presents the application of the on-load exciting current Park's Vector Approach for diagnosing permanent and intermittent turn-to-turn winding faults in operating power transformers. First, an experimental investigation of the behaviour of the transformer under the occurrence of both permanent and intermittent winding faults is presented. Finally, experimental test results demonstrate the effectiveness of the proposed diagnostic technique, which is based on the on-line monitoring of the on-load exciting current Park's Vector patterns.

KEYWORDS
Transformers, winding insulation faults, Park's Vector Approach.

INTRODUCTION

Power transformers are essential devices in a transmission and distribution system. Failure of a power transformer may cause a break in power supply and loss of profits. Therefore, it is of great importance to detect incipient failures in power transformers as early as possible, so that they can be switched off safely and improve the reliability of power systems (Wang, 2003).

The most difficult transformer winding fault for which to provide protection is the fault that initially involves only one turn (IEEE Standard C37.91, 2000). Initially, the insulation breakdown leads to internal arcing, which results into a low current, high impedance fault (Barkan et al, 1976). Usually, this incipient inter-turn insulation failure does not draw sufficient current from the line to operate an ordinary overload circuit-breaker or even more sensitive balanced protective gear (Stigant and Franklin, 1973; Raux et al, 1989). This turn-to-turn fault will then progress, with random propagation speed, involving additional turns and layers, leading to a high current, low impedance fault, (Plummer et al, 1995; Lunsford and Tobin, 1997). The transformer will, in fact, be disconnected from the line automatically when the fault has extended to such degree as to embrace a considerable portion of the affected winding (Stigant and

Franklin, 1973).

Previous research, concerning the use of the Park's Vector Approach, has demonstrated the effectiveness of this non-invasive technique for diagnosing malfunctions in operating three-phase induction motors, power electronics and adjustable speed drives (Cardoso, 1997). Preliminary experimental results, presented in (Cardoso and Oliveira, 1999), concerning the use of the supply current Park's Vector Approach, have also demonstrated the effectiveness of this technique for diagnosing the occurrence of inter-turn insulation faults in the windings of operating three-phase transformers. The on-line diagnosis is based on identifying the appearance of an elliptic pattern, corresponding to the transformer supply current Park's Vector representation, whose ellipticity increases with the severity of the fault and whose major axis orientation is associated to the faulty phase. However, with this approach, it is difficult to discriminate between unbalanced loads and winding faults. To overcome this difficulty, an improved diagnostic technique was implemented (Oliveira, 2001; Oliveira et al., 2002), which consists in the analysis of the on-load exciting current Park's Vector pattern, and therefore unaffected by the transformer's load conditions. Additionally, the on-load exciting current Park's Vector Approach enhances the severity of the fault, as compared to the former diagnostic technique (Oliveira and Cardoso, 2004).

As stated above, the initial turn-to-turn insulation defect leads to an arcing fault, which is a dangerous form of a short-circuit, that may have a low current magnitude. Arcing faults usually cause a damage that is limited to the fault area, and pose a great danger to the transformer (Abed and Mohammed, 2007). When the voltage potential between the affected turns breaks down the insulation a spark discharge takes place. The arc ignition and extinction depends on this threshold voltage (Morante and Nicoletti, 1999; Wang, 2001), resulting on a fault of intermittent nature. The behaviour of the transformer winding currents under the occurrence of this type of fault should be clearly understood, in order to allow the detection of the failure in its incipient stage. Although many studies about transformer inter-turn winding short-circuits have been reported in the literature, there is a surprisingly lack of publications presenting experimental results of the behaviour of the transformer under the occurrence of intermittent insulation winding faults.

There are two main goals in this paper. One is to present experimental results to characterize the behaviour of the transformer under the occurrence of permanent and intermittent winding faults. The second goal is to apply the on-load exciting current Park's Vector Approach to diagnose these faults.

EXPERIMENTAL SETUP AND FAULT CHARACTERIZATION

For the experimental investigation a three-phase, two winding, three leg transformer, of 10.3 kVA, 230/132 V, was used. In each winding of the transformer there are five additional tappings connected to the coils, allowing for the introduction of shorted turns at several locations in the winding, as shown in Fig. 1, for the phase *R* of the transformer primary and secondary windings. In the results presented in this paper an *YNyn*0 winding connection and a balanced resistive load were used in the laboratory tests, Fig. 2.

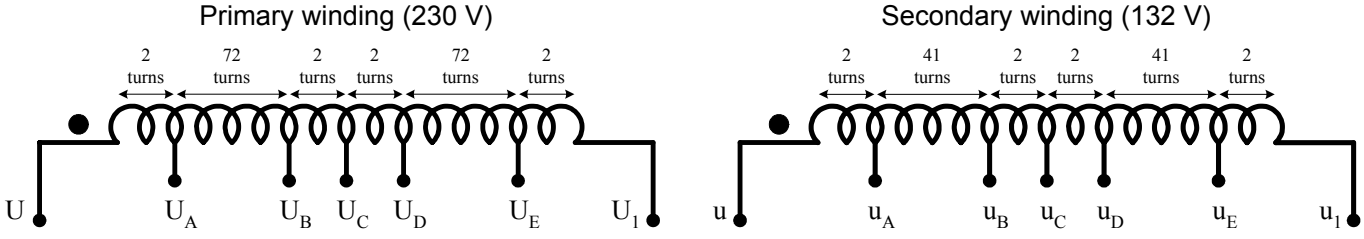

Fig. 1: Location of the tappings for transformer primary and secondary windings (phase R).

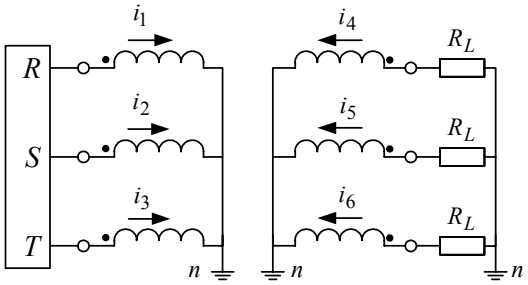

Fig. 2: Transformer *YNyn*0 winding connection.

Permanent Faults

The permanent faults are introduced in the transformer by connecting a shorting resistor at the terminals of the affected turns. The value of this resistor was chosen so as to create an effect strong enough to be easily visualised, but simultaneously big enough to limit the short-circuit current and thus protecting the test transformer from complete failure when the short is introduced.

If the fault occurs in the primary winding, the short-circuited turns act as an autotransformer load on the winding, as shown in Fig. 3(a), where R_{sh} represents the fault impedance. However, if the fault takes place on the secondary winding, the short-circuited turns act as an ordinary double winding load, Fig. 3(b), (Stigant and Franklin, 1973).

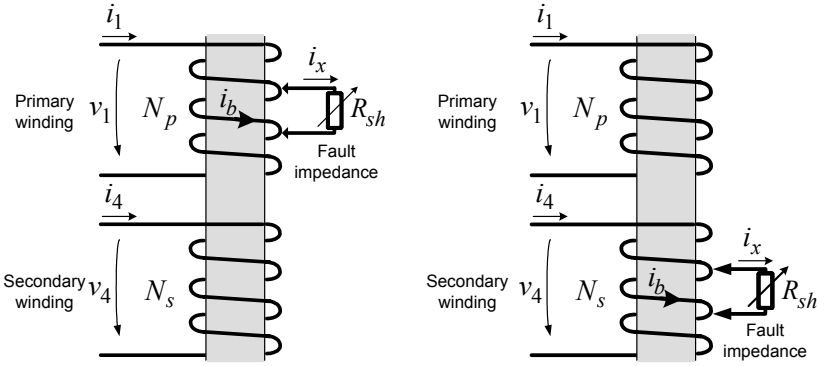

Fig. 3: Equivalent circuits for a fault occurring in the: (a) primary winding; (b) secondary winding, (phase *R*).

Fig. 4(a) presents the waveforms of the primary-side line currents, for the case of four permanent shorted turns in the phase *R* of the transformer primary winding (notation as per Fig. 2 and Fig. 3). The occurrence of primary-side inter-turn short-circuits leads to an increment in the magnitude of the current in the affected winding, as compared to a healthy condition, which results in an unbalanced system of primary currents. For this reason, the magnitude of the primary neutral current (i_{n1}=i_1+i_2+i_3), is also affected. In the presence of the primary winding inter-turn short-circuits, the secondary side currents do not present any relevant change as compared to the transformer's healthy operation, remaining an approximately balanced three-phase system, as shown in Fig. 4(b). The current waveform in the shorted turns, i_b, and the current waveform in the fault impedance, i_x, are shown in Fig. 4(c). The current i_b is approximately in phase opposition with i_1, due to the autotransformer action of the shorted turns. The current in the short-circuit auxiliary resistor, i_x, has a higher magnitude than i_b, since $i_x = i_1 - i_b$.

The input current in the affected winding can be divided in three terms:

$$i_1 = i'_4 + i_{exc1} + i'_x \tag{1}$$

where i'_4 is the secondary winding current referred to the primary-side, i_{exc1} is the excitation current and i'_x

is the current in fault impedance, also referred to the primary-side. Obviously, the first two terms are related with the healthy operation of the transformer, being the third a result of the shorted turns. The faulty current is reflected to the primary-side through the turns ratio between the number of shorted turns, N_b, and the total number of turns of the primary-side winding, N_p:

$$i'_x = i_x \times \frac{N_b}{N_p} \tag{2}$$

As a result, the increase in the magnitude of the primary-side winding current, due to an incipient insulation defect, with only a few turns involved, is small, even if the faulty current is large, and it is very likely that the fault remain undetected by the protection devices, until it progresses to a catastrophic failure. The severity of the fault depends not only on the number of shorted turns, but also on the value of the faulty current, which is limited by the fault impedance.

In the case of secondary-side winding faults, the additional load produced by the shorted turns also results into an increment in the magnitude of the correspondent primary-side winding current, as compared to a healthy condition, as shown in Fig. 5(a). Again, the line currents of the secondary-side do not suffer any significant alteration with the introduction of the defect, Fig. 5(b). However, with this type of fault, the current in the shorted turns is in phase with the line current of the affected winding, as shown in Fig. 5(c), and it takes larger values than the current in short-circuit auxiliary resistor.

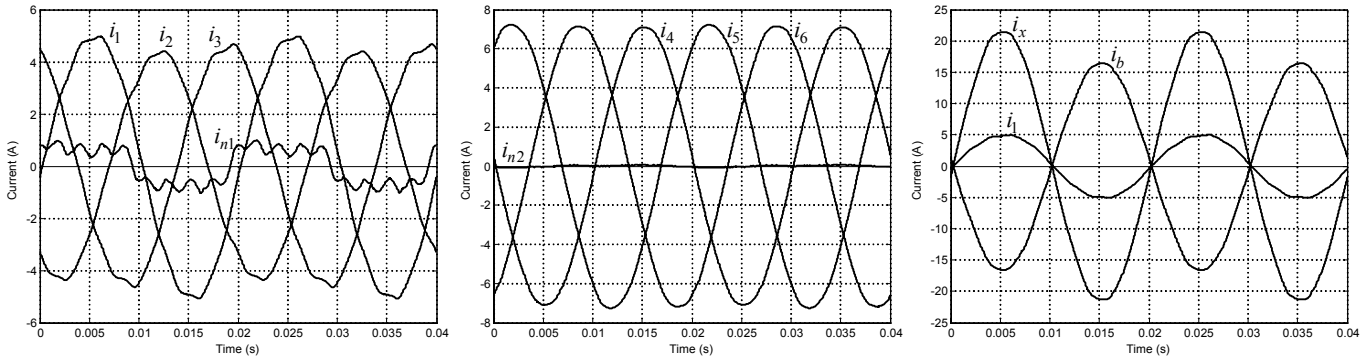

(a) (b) (c)

Fig. 4: Experimental test results for the case of a *YNyn*0 connection, a resistive balanced load and 4 permanent shorted turns in the primary winding (phase *R*): (a) primary-side currents waveforms; (b) secondary-side currents waveforms; (c) currents waveforms in the affected winding.

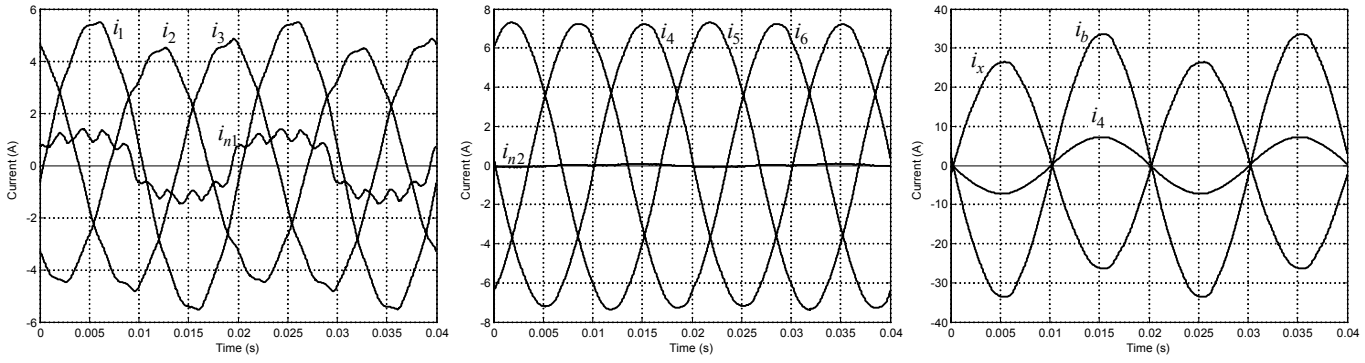

(a) (b) (c)

Fig. 5: Experimental test results for the case of a *YNyn*0 connection, a resistive balanced load and 4 permanent shorted turns in the secondary winding (phase *R*): (a) primary-side currents waveforms; (b) secondary-side currents waveforms; (c) currents waveforms in the affected winding.

The presence of the fault has the same end effect on the primary-side current, irrespective of whether the fault is located on primary or on the secondary-side, and Eqn. (1) and Eqn. (2) remain valid for both of these conditions.

Intermittent Faults

The arcing faults are introduced in the transformer by connecting a custom built power electronics board, at the terminals of the affected turns. Basically, the power electronics circuit consists of two modules, each one with an IGBT in series with a power diode, connected in anti-parallel, as shown in Fig. 6(a). The arc ignition and extinction depends on the threshold voltage, which is regulated by the firing angle and the conduction time (pulse width) of the IGBT's, Fig. 6(b). Again, an auxiliary shorting resistor was used, to maintain the faulty current within safe values.

Fig. 7(a) presents the arc current waveform, i_x, for the case of four intermittent shorted turns in the phase *R* of the transformer primary winding, maintaining the same load conditions and transformer winding connections mentioned above. In order to clearly visualize the transient phenomena, a pulse width of approximately 800 μs was chosen.

As in the case of permanent faults, the arc current is reflected to the primary-side through the turns ratio N_b/N_p, resulting in a pulse of relatively small magnitude in i_1, as shown in Fig. 7(b). Once again, the secondary-side currents do not present any significant change with the introduction of the defect.

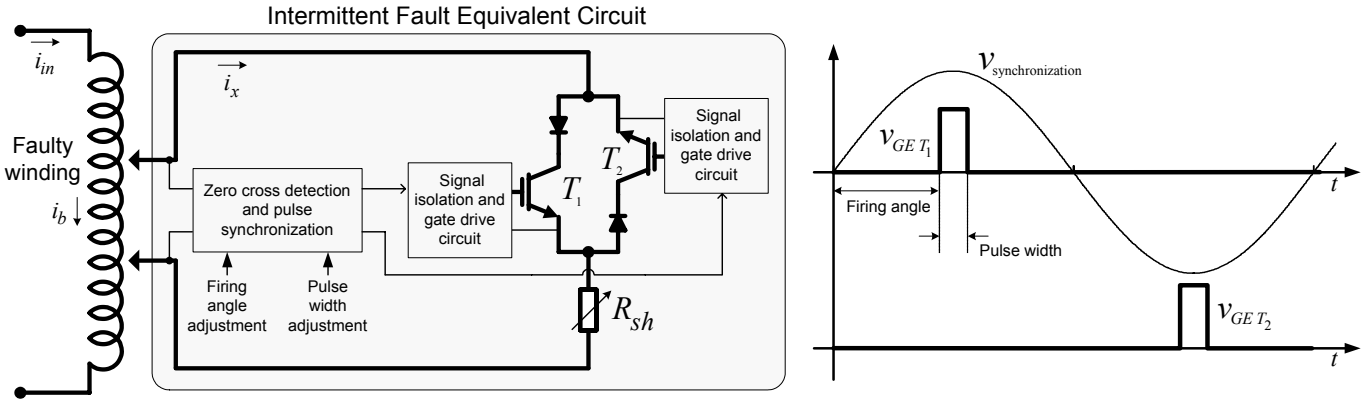

(a) (b)

Fig. 6: (a) Intermittent fault equivalent circuit with a power electronics board; (b) gate signals of the IGBT's.

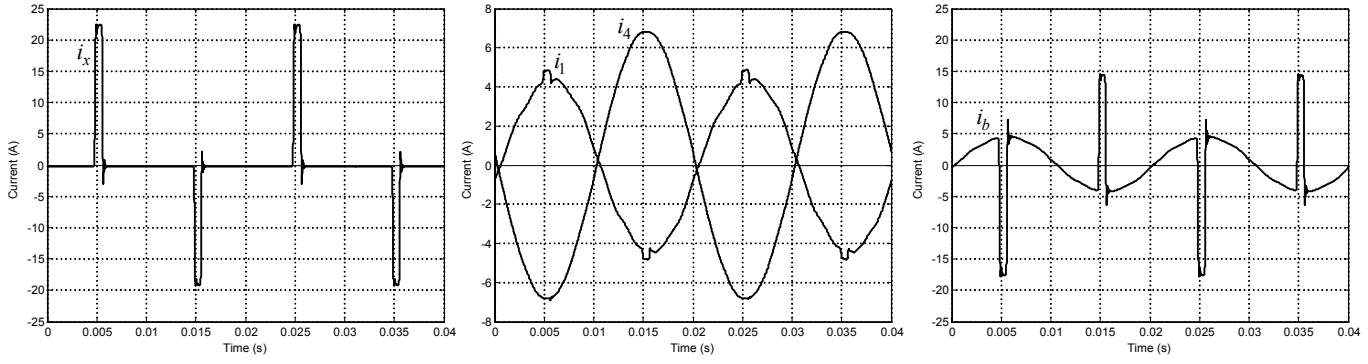

(a) (b) (c)

Fig. 7: Experimental test results for the case of a *YNyn*0 connection, a resistive balanced load and 4 intermittent shorted turns in the primary winding (phase *R*): (a) arc current waveform; (b) primary and secondary-side currents waveforms of the affected phase; (c) current waveform in the shorted turns.

The current waveform in the shorted turns is shown in Fig. 7(c). When i_x is zero, the current in the defected turns is equal to i_1. During the arc discharge, i_b presents a deep notch, since $i_b = i_1 - i_x$.

For the same aforementioned conditions, but now for the case of four intermittent shorted turns in the phase *R* of the transformer secondary winding, the current waveforms in the shorting resistor, in the primary and secondary-side windings of the affected phase and in the shorted turns are presented in Fig. 8(a), Fig. 8(b) and Fig. 8(c), respectively. In comparison with the previous test, the only significant difference is the current waveform in the shorted turns, which is now given by $i_b = i_4 - i_x$.

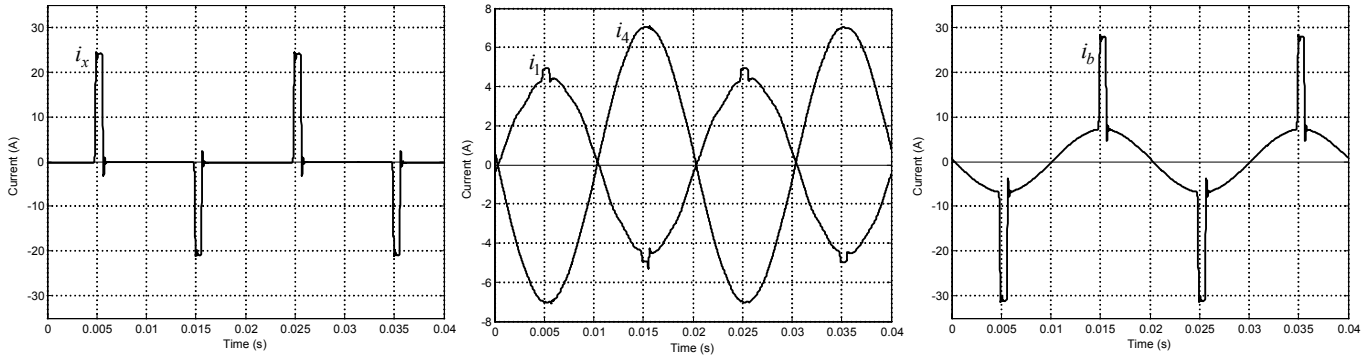

(a) (b) (c)

Fig. 8: Experimental test results for the case of a *YNyn*0 connection, a resistive balanced load and 4 intermittent shorted turns in the secondary winding (phase *R*): (a) arc current waveform; (b) primary and secondary-side currents waveforms of the affected phase; (c) current waveform in the shorted turns.

WINDING FAULTS DETECTION BY THE ON-LOAD EXCITING CURRENT PARK'S VECTOR APPROACH

The on-load exciting current waveforms are computed by adding the primary and secondary winding currents, both referred to the primary side. For the *YNyn*0 winding connection (Fig. 2) the on-load exciting currents are:

$$\begin{aligned} i_{e1} &= i_1 + i_4 \cdot N_s / N_p \\ i_{e2} &= i_2 + i_5 \cdot N_s / N_p \\ i_{e3} &= i_3 + i_6 \cdot N_s / N_p \end{aligned} \tag{3}$$

where N_p and N_s are the numbers of turns of primary and secondary windings, respectively. For the case of other transformer connections, the on-load exciting currents can be obtained by using the same basic principle, but with slightly different computations (Oliveira, 2001; Oliveira et al., 2002).

The transformer on-load exciting current Park's Vector components (i_{eD}, i_{eQ}) are:

$$i_{eD} = \left(\sqrt{2}/\sqrt{3}\right)\, i_{e1} - \left(1/\sqrt{6}\right)\, i_{e2} - \left(1/\sqrt{6}\right)\, i_{e3} \tag{4}$$

$$i_{eQ} = \left(1/\sqrt{2}\right)\, i_{e2} - \left(1/\sqrt{2}\right)\, i_{e3} \tag{5}$$

Under ideal conditions, the three-phase on-load exciting currents lead to a Park's Vector with the following components:

$$i_{eD} = \left(\sqrt{6}/2\right)\, \hat{I}_M\, \sin\left(\omega t\right) \tag{6}$$

$$i_{eQ} = \left(\sqrt{6}/2\right)\, \hat{I}_M\, \sin\left(\omega t - \pi/2\right) \tag{7}$$

where $\hat{I}_M$ is the maximum value of the on-load exciting current (A), ω is the angular supply frequency (rad/s) and t is the time variable (s). The corresponding representation is a circular locus centered at the origin of the coordinates. Under abnormal conditions Eqn. (6) and Eqn. (7) are no longer valid and consequently the observed picture differs from the reference pattern.

Fig. 9(a) presents the on-load exciting current Park's Vector pattern for the case of an *YNyn*0 winding connection and for a healthy operation of the transformer. This pattern differs from the circular locus expected for an ideal situation, due to, among others, the non-linear behaviour and asymmetry of the magnetic circuit. This is a well known phenomenon, which is revealed by the unbalanced and distorted nature of the exciting currents obtained from any three-phase no-load test (Oliveira and Cardoso, 2004). In fact, the exciting current Park's Vector pattern, obtained at no-load conditions, presents the same characteristics, as shown in Fig 9(b).

The occurrence of primary-side permanent winding faults manifests itself in the deformation of the on-load exciting current Park's Vector pattern corresponding to a healthy condition, leading to an elliptic representation, whose ellipticity increases with the severity of the fault and whose major axis orientation is associated to the faulty phase. This can be seen in Fig. 10, which presents the on-load exciting currents Park's Vector patterns, for different numbers of shorted turns in the primary windings, located in each one of the three phases. For all the cases in Fig. 10, the auxiliary short-circuit resistor was adjusted in order to limit the magnitude of the faulty current, $\hat{I}_x$, to the rated magnitude of the current in the affected winding, $\hat{I}_{1n}$.

Similar conclusions, concerning the on-load exciting current Park's Vector patterns, can be drawn for the occurrence of secondary-side inter-turn short-circuits (Oliveira, 2001).

For the case of intermittent faults, the same operating philosophy is applied, but a spiked on-load exciting current Park's Vector pattern is obtained. As shown in Fig. 11, the faulty phase is now detected by the pulsed pattern orientation. Fig. 12 presents the evolution of the on-load exciting current Park's Vector pattern when the magnitude of the faulty current is increased from $0.5 \times \hat{I}_{1n}$ to $1.5 \times \hat{I}_{1n}$. The severity of the fault is directly related with the magnitude of the pulsed pattern. Additionally, the results clearly indicate that the proposed diagnostic technique is sensitive to low level faults.

Other experimental and simulated tests carried out for different types of the transformer windings connection, fault location and load conditions lead to similar conclusions to the ones presented before (Oliveira, 2001; Oliveira and Cardoso, 2001; Oliveira and Cardoso, 2002; Oliveira et al., 2002).

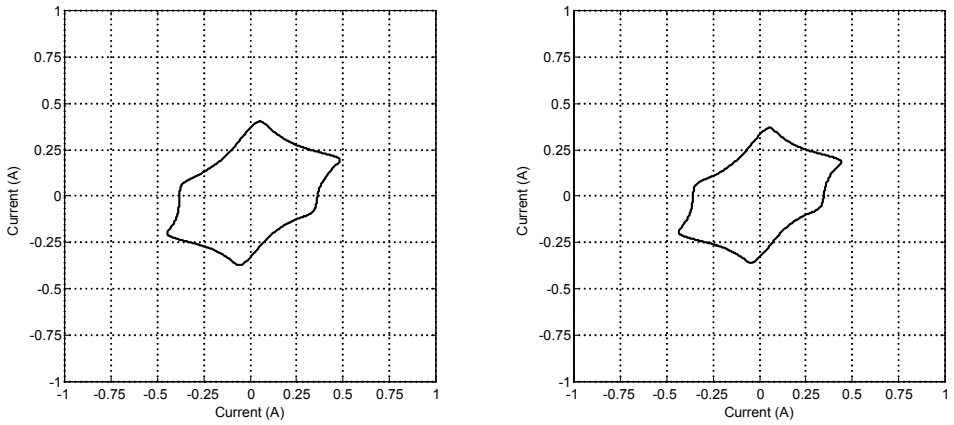

(a) (b)

Figure 9: On-load exciting current Park's Vector pattern (a) and no-load exciting current Park's Vector pattern (b), for the case of an *YNyn*0 connection and healthy operating conditions.

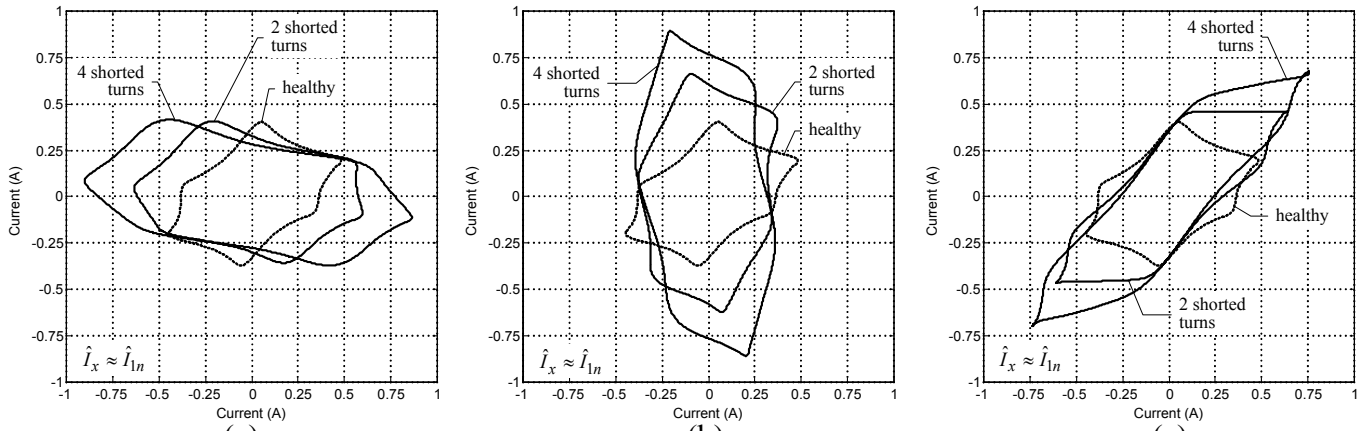

Fig. 10: On-load exciting current Park's Vector patterns for the case of a *YNyn*0 connection and a balanced resistive load, with several percentages of permanent shorted turns in the primary windings and for different faulty phases: (a) phase *R*; (b) phase *S*; (c) phase *T*.

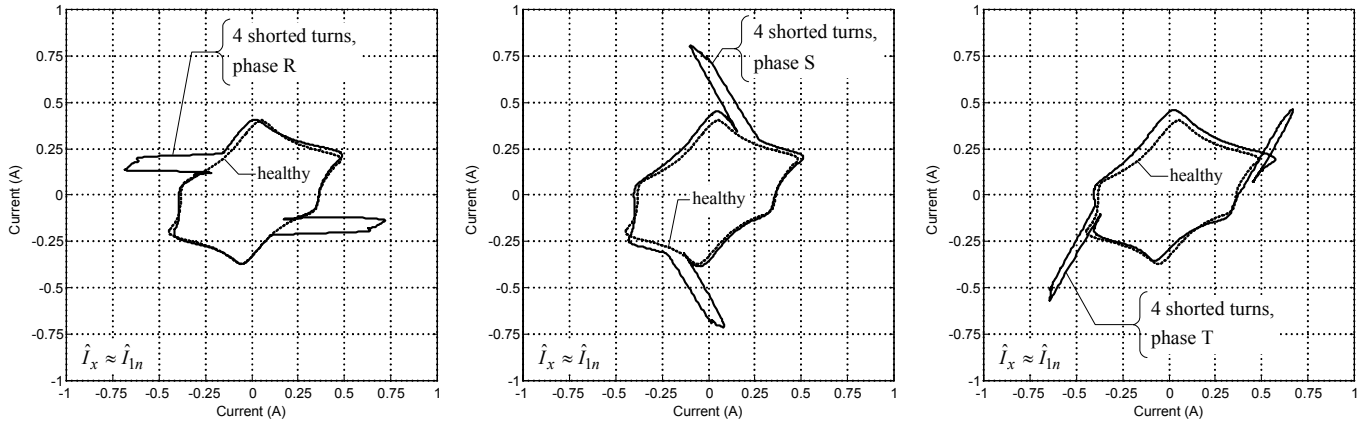

Fig. 11: On-load exciting current Park's Vector patterns for the case of a *YNyn*0 connection and a balanced resistive load, with four intermittent shorted turns in the primary windings and for different faulty phases: (a) phase *R*; (b) phase *S*; (c) phase *T*.

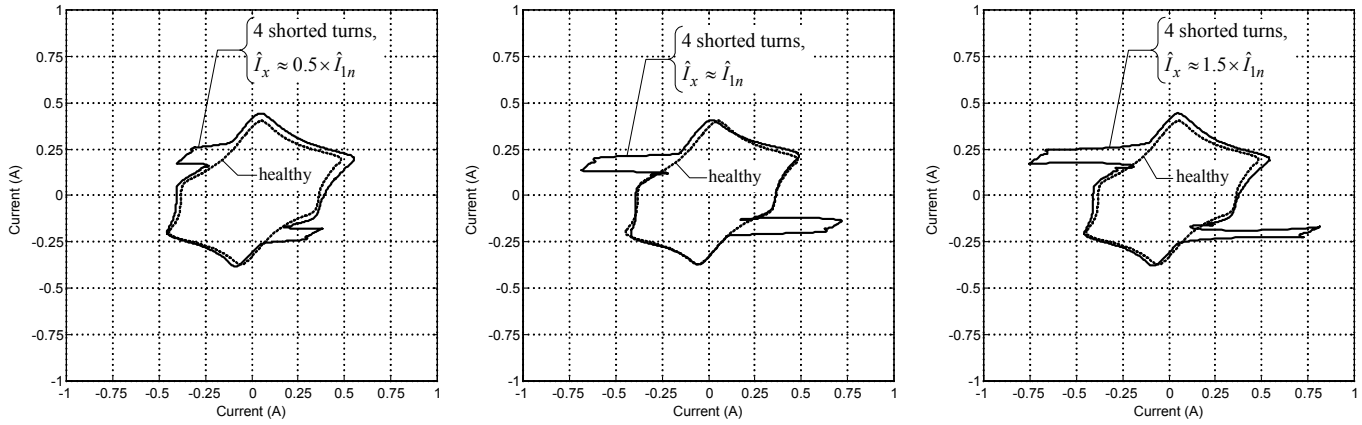

Fig. 12: On-load exciting current Park's Vector patterns for the case of a *YNyn*0 connection and a balanced resistive load, with four intermittent shorted turns in the primary winding of phase R and for different values of the magnitude of the pulsed faulty current, $\hat{I}_x$ (in terms of the rated magnitude of the current in the affected winding, $\hat{I}_{1n}$): (a) $\hat{I}_x \approx 0.5 \times \hat{I}_{1n}$; (b) $\hat{I}_x \approx \hat{I}_{1n}$; (c) $\hat{I}_x \approx 1.5 \times \hat{I}_{1n}$.

CONCLUSIONS

This paper presents the application of the on-load exciting current Park's Vector Approach for diagnosing the occurrence of intermittent inter-turn short-circuits in the windings of operating three-phase transformers, which consists in the analysis of the on-load exciting current Park's Vector patterns. The on-line diagnosis of winding intermittent faults is based on identifying the appearance of a pulsed pattern, corresponding to the transformer on-load exciting current Park's Vector representation, whose pulse magnitude increases with the severity of the fault and whose major axis orientation is associated to the faulty phase. The proposed on-line diagnostic technique combines the advantages of two well known methods:

- the Park's Vector Approach, which assemble the three-phase system in only one quantity;
- the on load exciting current, which enhances the severity of the fault, giving an increased sensitivity about the condition of the transformer.

Experimental test results were presented, for both permanent and intermittent winding insulation faults, which demonstrate the effectiveness of the diagnostic technique.

REFERENCES

Abed, N. Y. and Mohammed, O.A. (2007) "Modeling and characterization of transformers internal faults using finite element and discrete wavelet transforms", IEEE Transactions on Magnetics, Vol. 43, No. 4, pp. 1425-1428.

Barkan, P.; Damsky, B. L.; Ettlinger, L. F. and Kotski, E. J. (1976) "Overpressure phenomena in distribution transformers with low impedance faults: experiment and theory", IEEE Transactions on Power Apparatus and Systems, Vol. 95, No. 1, pp. 37-48.

Cardoso, A. J. M. (1997) "The Park's Vector Approach: a general tool for diagnostics of electrical machines, power electronics and adjustable speed drives", Record of the 1997 IEEE International Symposium on Diagnostics for Electrical Machines, Power Electronics and Drives, Carry-le-Rouet, France, pp. 261-269.

Cardoso, A. J. M. and Oliveira, L. M. R. (1999) "Condition monitoring and diagnostics of power transformers", International Journal of COMADEM, Vol. 2, No. 3, pp. 5-11.

IEEE Standard C37.91 (2000) "IEEE Guide for Protective Relay Applications to Power Transformers", Chapter 5.

Lunsford, J. M. and Tobin, T. J. (1997) "Detection of and protection for internal low-current winding faults in overhead distribution transformers", IEEE Transactions on Power Delivery, Vol. 12, No. 3, pp. 1241-1249.

Morante, M. G. and Nicoletti, D. W. (1999) "A wavelet-based differential transformer protection", IEEE Transactions on Power Delivery, Vol. 14, No. 4, pp 1351-1359.

Oliveira, L. M. R. (2001) "Development and implementation of a digital model for transformer winding fault studies – an introduction to a new diagnostic method", (in Portuguese), Thesis (M.Sc.), University of Coimbra, Portugal.

Oliveira, L. M. R. and Cardoso, A. J. M. (2001) "A coupled electromagnetic transformer model for the analysis of winding inter-turn short-circuits" Record of the 2001 IEEE International Symposium on Diagnostics for Electrical Machines, Power Electronics and Drives, Grado, Italy, pp. 367-372.

Oliveira, L. M. R. and Cardoso, A. J. M (2002) "On-line diagnostics of transformer winding insulation failures, by Park's Vector Approach", Proceedings of the 9th International Electrical Insulation Conference (INSUCON 2002), Berlin, Germany, pp. 16-21.

Oliveira, L. M. R.; Cardoso, A. J. M. and Cruz, S. M. A. (2002) "Transformers on-load exciting current Park's Vector Approach as a tool for winding faults diagnostics", Conference Record of the 15th International Conference on Electrical Machines (ICEM 2002), Brugge, Belgium, 6 pp., CD-ROM.

Oliveira, L. M. R. and Cardoso, A. J. M. (2004) "Incipient turn-to-turn winding fault diagnosis of power transformers by the on-load exciting current Extended Park's Vector Approach", Proc. Of the Advanced Research Workshop on Modern Transformers (ARWtr04), Vigo, Spain, pp. 134-139.

Plummer, C. W.; Goedde, G. L.; Petit, E. L.; Godbee, J. S. and Hennessey, M. G. (1995) "Reduction in distribution transformer failures rates and nuisance outages using improved lightning protection concepts", IEEE Transactions on Power Delivery, Vol. 10, No. 2, pp. 768-777.

Raux, C.; Leconte, C. and Gibert, T. (1989) "Resistance of transformers to internal faults: synthesis of experimental results", 10th International Conference on Electricity Distribution (CIRED 1989), pp. 71-75.

Stigant, S. A. and Franklin, A. C. (1973) The J&P Transformer Book, 10th Edition, Newnes--Butterworths, London.

Wang, H. (2001) "Models for short circuit and incipient internal faults in single-phase distribution transformers", Thesis (PhD), Texas A&M University.

Wang, M. (2003) "A novel extension method for transformer fault diagnosis", IEEE Transactions on Power Delivery, Vol. 18, No. 1, pp. 164-169.